KECK-I MOSFIRE SPECTROSCOPY OF THE $z \sim 12$ CANDIDATE GALAXY UDFj-39546284[*]

P. CAPAK[1], A. FAISST[2], J. D. VIEIRA[3], S. TACCHELLA[2], M. CAROLLO[2], AND N. Z. SCOVILLE[3]
[1] Spitzer Science Center, 314-6 Caltech, Pasadena, CA 91125, USA
[2] Institute for Astronomy, Swiss Federal Institute of Technology (ETH Zurich), CH-8093 Zurich, Switzerland
[3] California Institute of Technology, 314-6 Caltech, Pasadena, CA 91125, USA

ABSTRACT

We report the results of deep (4.6 hr) H-band spectroscopy of the well studied $z \sim 12$ H-band dropout galaxy candidate UDFj-39546284 with MOSFIRE on Keck-I. These data reach a sensitivity of 5–10×10^{-19} erg s^{-1} cm^{-2} per 4.4 Å resolution element between sky lines. Previous papers have argued that this source could either be a large equivalent width line emitting galaxy at $2 < z < 3.5$ or a luminous galaxy at $z \sim 12$. We find a 2.2σ peak associated with a line candidate in deep *Hubble Space Telescope* Wide-Field Camera 3 Infrared grism observations, but at a lower flux than expected. After considering several possibilities, we conclude these data cannot conclusively confirm or reject the previous line detection, and significantly deeper spectroscopic observations are required. We also search for low-redshift emission lines in 10 other $7 < z < 10$ z, Y, and J-dropout candidates in our mask and find no significant detections.

Key words: galaxies: formation – galaxies: high-redshift – line: identification

Online-only material: color figures

1. INTRODUCTION

Deep photometric surveys with the *Hubble Space Telescope* (*HST*) are revolutionizing our knowledge of the star-forming galaxy population at the epoch of hydrogen re-ionization, only a few hundred million years after the big bang. Hundreds of candidate $z \sim 7$–8 galaxies have now been discovered using the Lyman break galaxy (LBG or "dropout") technique using newly available *HST* Wide-Field Camera 3 Infrared (WFC3-IR) data (Bouwens et al. 2010; Oesch et al. 2010; McLure et al. 2013; Ellis et al. 2013). Recently, this technique has been pushed to $z \sim 12$ by using hundreds of *HST* orbits to probe to unprecedented depths in the Hubble Ultra-Deep Field 2012 (HUDF12; Ellis et al. 2013).

The LBG or "dropout" technique relies on absorption by intervening neutral hydrogen below the Lyman limit at 912 Å and Lyα at 1216 Å to create a strong spectral break that differentiates high- and low-redshift galaxies using only broadband photometry. This technique was first introduced in the 1980s and 1990s (Cowie 1988; Steidel et al. 1996) and was broadly adopted as the main technique for finding candidate distant sources once it was shown to be effective spectroscopically on large samples at $z \sim 3$–4 (Steidel et al. 1999, 2002) and then deployed at ever higher redshifts (Iwata et al. 2003; Ouchi et al. 2004; Bouwens et al. 2007). The current frontier is to use the near-infrared WFC3/IR Hubble Ultra-Deep Field data for "J- and H-dropout" galaxies at redshifts $z \sim 8$–12 and has led to a handful of tentative detections, most notably the source UDFj-39546284, a candidate $z \sim 11.9$ galaxy (Ellis et al. 2013) previously claimed to be at $z \sim 10.3$ (Bouwens et al. 2011a; Oesch et al. 2012). If confirmed to be at such high redshifts, even this single galaxy would be of paramount importance to probe the physics of the earliest phases of galaxy formation,

and to quantify how star-forming galaxies contribute to the re-ionization of the Universe (Robertson et al. 2010; Bouwens et al. 2011a; Oesch et al. 2012).

However, spectroscopic redshifts are fundamental to ascertain the true redshifts of candidate high-z LBGs. At $z > 4$, the application of the dropout technique has lead to notably diverse results (Iwata et al. 2003; Ouchi et al. 2004; Bouwens et al. 2007; van der Burg et al. 2010) with only limited samples being spectroscopically confirmed (Vanzella et al. 2009; Stark et al. 2010; Mallery et al. 2012), and the vast majority of spectroscopy failing to detect anything significant. For example, Stark et al. (2010) and Vanzella et al. (2009), two of the largest spectroscopic samples at $z > 4$ to date, confirm less than half of their targeted objects. This is particularly problematic at $z > 6$ where exotic objects can contaminate the dropout selection (Capak et al. 2011).

A growing body of evidence suggests extreme line emitters and unusual evolved galaxies at $z \sim 2$ are a contaminant in $z > 7$ LBG selections (Atek et al. 2011; Capak et al. 2011; Hayes et al. 2012). In published spectroscopic studies of $z > 7$ galaxies, the vast majority of results are null, with a large fraction of detected objects placed at $z < 3$ (Vanzella et al. 2011; Capak et al. 2011; Caruana et al. 2012; Hayes et al. 2012; Ono et al. 2012; Bunker et al. 2013). The null results combined with the type of contamination is worrying because it is from a poorly understood population of objects and so is difficult to include in the simulations required to quantify LBG selection criteria (Capak et al. 2011). In the near term, this highlights the need for deep spectroscopic studies at $6 < z < 8$ where current spectrographs can hope to confirm existing high-z candidates and characterize contaminating populations. In the longer run, the James Web Space Telescope and 30 m class ground-based telescopes will be necessary to obtain the requisite spectroscopic samples at $z > 8$ and faint fluxes needed to understand these populations.

UDFj-39546284 has been well studied by many authors and is only detected in the F160W H-band filter with *HST* WFC3-IR, even though the deepest data currently available exists at both
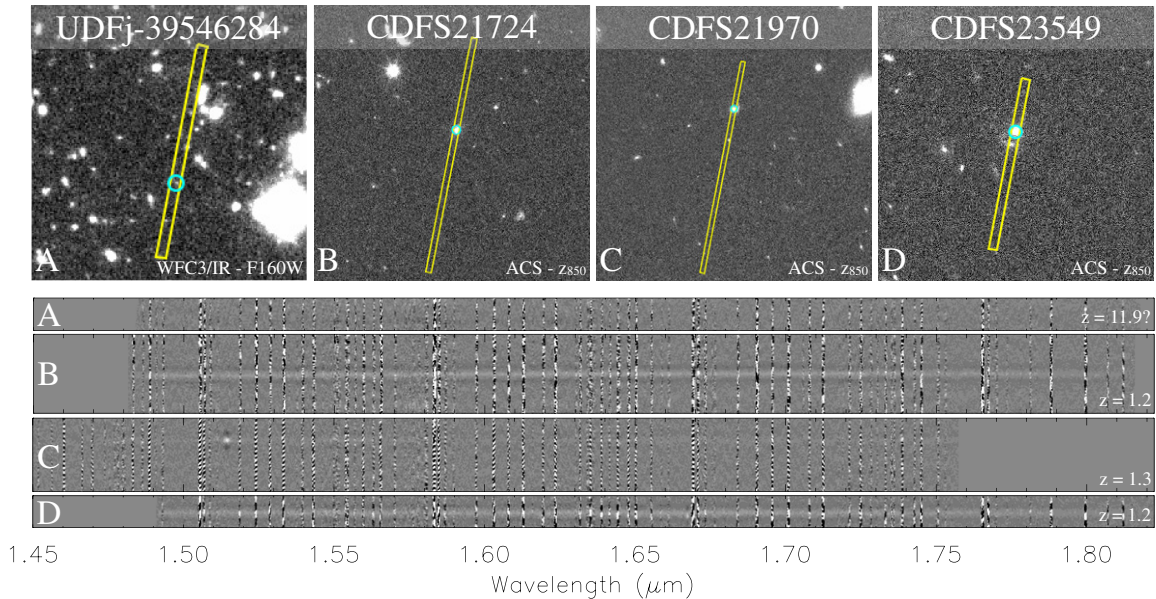
Figure 1. Image cutouts and the two-dimensional MOSFIRE spectra around UDFj-39546284 (A) and three other bright objects are shown. The MOSFIRE slit positions are marked in yellow and the objects highlighted with a cyan circle. Analysis of the bright compact-object spectra CDFS21724 (B) indicates we are losing no more than 10% of the flux due to mask misalignment. The strong line visible in CDFS21970 (C) is Hα at $z = 1.3089$. A summary of these and other objects in the mask is given in Table 1.

(A color version of this figure is available in the online journal.)

bluer and redder wavelengths. It was first reported by Bouwens et al. (2011a), who originally claimed it was at $z \sim 10$. Ellis et al. (2013) recently improved the depth of the HUDF F160W and the F105W images by 0.2 and 0.5 mag, respectively, and added deep F140W imaging which overlaps the blue half of F160W. This new data (HUDF12) favors UDFj-39546284 being at $z = 11.9$, but still allows the possibility that it could be a strong line emitter at $2 < z < 3.5$. Subsequently, Brammer et al. (2013) reported a 2.7σ line detection at 15990 ± 40 Å with a flux of $3.5 \pm 1.3 \times 10^{-18}$ erg s^{-1} cm^{-2} based on 40,500 s of *HST* WFC3-IR $R \sim 140$ grism spectroscopy. However, this detection required significant modeling of the data to remove overlapping spectra and background artifacts. Subsequent re-analysis of the deeper imaging and spectroscopic data by Bouwens et al. (2013) now lead them to the conclusion that the galaxy is more likely at $z \sim 2$ than $z \sim 10$–12 based on the argument that the galaxy would be unusually luminous if actually at $z \sim 12$.

If UDFj-39546284 is at low redshift, then the photometric constraints indicate it must be a young blue galaxy with strong line emission that has a line flux of $\sim 3 \times 10^{-18}$ erg s^{-1} cm^{-2} for a typical dwarf galaxy velocity dispersion (Ellis et al. 2013; Brammer et al. 2013; Bouwens et al. 2013). Furthermore, the line reported by Brammer et al. (2013) falls in a region largely free of sky lines and so can be confirmed by ground-based spectroscopy which has significantly higher sensitivity and spectral resolution.

In this Letter, we present $R \sim 3630$ *H*-band spectroscopy of UDFj-39546284 with the MOSFIRE multi-object infrared spectrograph (McLean et al. 2010, 2012) on the Keck-I telescope, reaching two to three times the sensitivity of the WFC3 grism spectroscopy between sky lines. This new instrument saw its first light in 2012 April, and provides a substantial boost in sensitivity relative to previous facilities for studies of very faint distant galaxies. Its high-multiplexing of up to 46 adjustable slitlets over a field of view of $6' \times 6'$ enables the simultaneous acquisition of scores of individual sources. In addition to

UDFj-39546284, we give a summary of the results from other objects on our slit mask in Table 1.

We adopt a cosmological model with $\Omega_\Lambda = 0.7$, $\Omega_M = 0.3$, and $h = 0.7$ and magnitudes in the AB system.
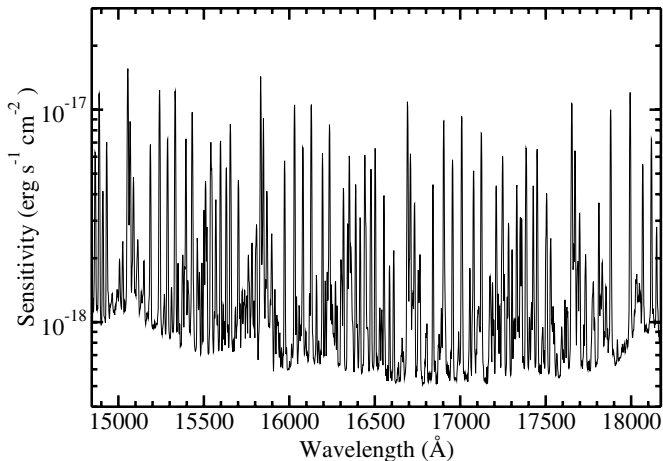
2. DATA

Data were collected on the nights of 2013 January 15 and 16 using the MOSFIRE instrument on the Keck-I telescope. Conditions were photometric on both nights, with a median seeing of $1''.2$. The instrument was configured with the *H*-band grating, $0''.7$ slit widths, 180 s exposures, and 16 Multiple Correlated Double Samples. The telescope was nodded by $\pm 1''.25$ between observations with 44 exposures taken on January 15, and 48 on January 16, yielding a total exposure time of 4.6 hr on the mask.

We used bright Two Micron All Sky Survey (2MASS) stars for alignment, but noted a significant $\sim 1''$ offset between the 2MASS and HUDF12 astrometry, which was corrected before generating the mask. We verified that the alignment stars and galaxies in the HUDF12 were on the same astrometric system by comparing the astrometry of the alignment stars and galaxies on the HUDF12 images and the surrounding *HST* Advanced Camera for Surveys images which covered a wider area. Based on repeated alignment exposures taken every one to two hours during both nights, the mask was aligned to better than $0''.1$ during the observations. Finally, to verify the mask was properly aligned, relatively bright objects were placed on slits around the mask and their flux checked against the expectations from photometry (see Figure 1).

The data were reduced using the MOSFIRE python reduction package which subtracts nodded pairs of images, then shifts and co-adds the exposures using a sigma-clipped noise weighted mean. The argon and neon arc lamps along with sky lines were used for wavelength calibration. We generated a combined image of all 92 (4.6 hr) exposures as well as combinations including only three-fourths of the data (3.45 hr) to test the
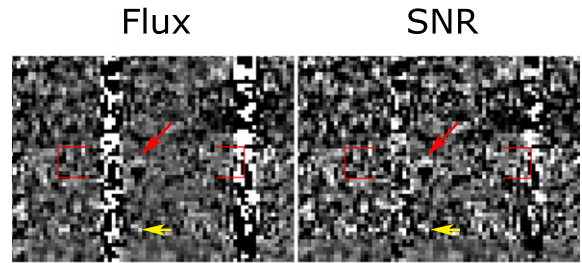
Table 1
Targeted Objects

ID	R.A.	Decl.	H_{AB}[a]	Comments
CDFS21724[b]	03^{h}32^{m}35^s.636	−27^{d}43^{m}10^s.16	20.49	low-z, continuum S/N = 9.6
CDFS21970[b]	03^{h}32^{m}35^s.972	−27^{d}48^{m}50^s.40	21.04	low-z, continuum S/N= 1.75, strong H$_\alpha$ line
CDFS23549[b]	03^{h}32^{m}38^s.107	−27^{d}44^{m}32^s.59	20.41	low-z, continuum S/N= 9.2
UDFj-39546284[c]	03^{h}32^{m}39^s.54	−27^{d}46^{m}28^s.4	29.3	$z \sim 12$ J drop, no detection
UDF12-4106-7304[c]	03^{h}32^{m}41^s.06	−27^{d}47^{m}30^s.4	29.7	$z \sim 10$ J drop, no detection
UDF12-3947-8076[c]	03^{h}32^{m}39^s.47	−27^{d}48^{m}07^s.6	29.0	$z \sim 10$ J drop, no detection
UDFj-43696407[c]	03^{h}32^{m}43^s.69	−27^{d}46^{m}40^s.7	29.5	$z \sim 10$ J drop, no detection
UDFj-35427336[c]	03^{h}32^{m}35^s.42	−27^{d}47^{m}33^s.6	29.6	$z \sim 10$ J drop, no detection
UDFy-33436598[c]	03^{h}32^{m}33^s.43	−27^{d}46^{m}59^s.8	29.4	$z \sim 8$ Y drop, no detection
UDF12-3858-6150[d]	03^{h}32^{m}38^s.58	−27^{d}46^{m}15^s.0	29.9	$z \sim 8$ Y drop, no detection
UDF12-3939-7040[d]	03^{h}32^{m}39^s.39	−27^{d}47^{m}04^s.0	28.9	$z \sim 8$ Y drop, no detection
UDF12-4057-6436[d]	03^{h}32^{m}40^s.57	−27^{d}46^{m}43^s.6	28.7	$z \sim 7$ z drop, no detection
UDF12-3817-7327[d]	03^{h}32^{m}38^s.17	−27^{d}47^{m}32^s.7	30.3	$z \sim 7$ z drop, no detection
UDF12-3853-7519[d]	03^{h}32^{m}38^s.53	−27^{d}47^{m}51^s.9	29.7	$z \sim 7$ z drop, no detection

Notes.
[a] WFC3-IR F160W for all source names starting with UDF, and ISAAC *H* for those starting with CDFS.
[b] Cardamone et al. (2010).
[c] Ellis et al. (2013).
[d] Bouwens et al. (2011b); Schenker et al. (2013).

Figure 2. Measured 1σ sensitivity per 4.4 Å resolution element at the position of UDFj-39546284 is plotted. The measured sensitivity is consistent with that predicted by the instrument exposure time calculator. Note that we should be able to detect a $\sim 3 \times 10^{-18}$ erg s^{-1} cm^{-2} line implied by the photometry at several sigma between sky lines.

Figure 3. Flux and signal-to-noise (S/N) map of the region around the potential detection reported by Brammer et al. (2013). The region allowed by Brammer et al. (2013) is marked by the red brackets, and the potential 2.2σ detection in our data is marked by a red arrow. The region used to subtract the sky from the negative spot below the detection is indicated with a yellow arrow; note the positive fluctuation at this position.

(A color version of this figure is available in the online journal.)

robustness of the reductions, noise estimates, and for temporal variations.

Flux calibration was accomplished by taking spectra of the white dwarf spectrophotometric standard star GD71. The standard star was observed with a pair of exposures using an identical setting to the science observations and reduced in the same way as the science data. The well detected spectra of the compact, 0.''36 FWHM in the *HST* F160W images, $z = 1.22$ galaxy CDFS21724 was used to verify our spectrophotometric calibration, slit loss, and noise estimates by comparing this spectra to the ISAAC *H*-band flux from the MUSYC catalog (Cardamone et al. 2010), the GOODS-S Early Release Science F160W flux, and the noise estimates from the MOSFIRE exposure time calculator. Based on the CDFS21724 spectra, additional slit losses due to object extent and mask misalignment are estimated to be 5%–10% greater than estimated for the standard star. The noise measured in CDFS21724 between 15920 and 15950 Å is 8.5×10^{-19} erg s^{-1} cm^{-2} per 4.4 Å

resolution element, which is consistent with the estimate of 8.1×10^{-19} erg s^{-1} cm^{-2} from the exposure time calculator once the slit losses of 48% due to poor seeing, and 10% due to object extension and mask alignment are taken into account. Two other bright objects, CDFS21970 and CDFS23549, were also placed on the mask to verify the throughput and resulted in the expected signal to noise, but were not used for quantitative analysis because of a strong emission line (CDFS21970) and complex morphology (CDFS23549) which made a comparison to UDFj-39546284 more difficult. The estimated sensitivity per resolution element is plotted in Figure 2 and results for the alignment galaxies and high-z spectra are given in Table 1.

To find potential emission lines, we used SExtractor to automatically search for groups of nine pixels above 1σ with no smoothing yielding a $>3\sigma$ net detection, as well as visually inspecting the spectra at the expected position of UDFj-39546284. We find no robust line detections, but do find a 2.2σ peak at 15985.5 ± 4.4 Å with a flux of $1.4 \pm 0.6 \times 10^{-18}$ erg s^{-1} cm^{-2} in a 6 pixel diameter aperture (Figure 3), consistent at the 1.5σ level with the wavelength and flux reported in Brammer et al. (2013). We also measured the line flux using an optimal extraction assuming a 1.''2 Gaussian FWHM and found the same result. This corresponds to $70\% \pm 30\%$ of the measured broadband flux,
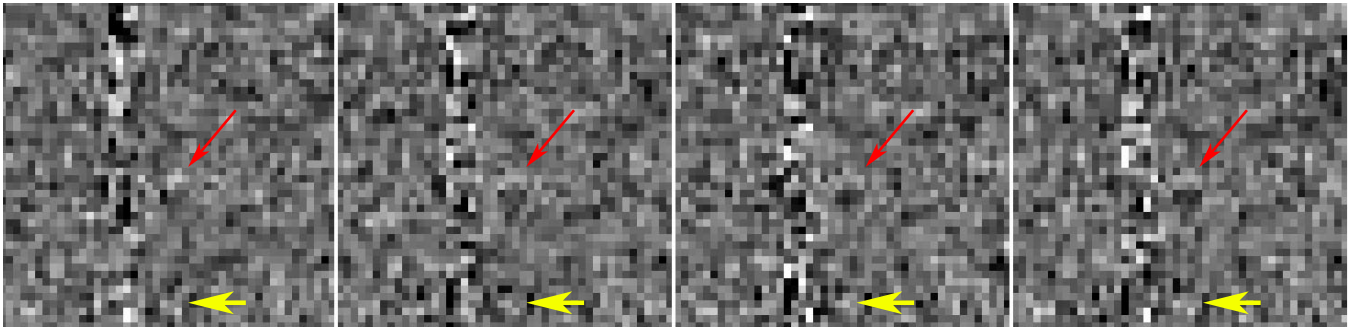
Figure 4. Signal-to-noise maps of the area around the possible line detection with a quarter of the data removed in each reduction. Note that the possible line detection shown in Figure 3 is present in all four reductions with a significance of 1.3σ–2.6σ consistent with the expected noise. In contrast, the negative spot below the detection varies significantly, indicating it is due to noise. The regions used to subtract the sky from the negative spot below the detection is indicated with a yellow arrow.

(A color version of this figure is available in the online journal.)

and would correspond to an observed frame equivalent width of ~6400 Å.

The peak is present in all of the reductions which include only three-fourths of the data (at reduced significance; see Figure 4) and measurement of the flux at the positions of the expected negative images due to the dithering return a consistent negative flux, increasing the reliability of the detection. No known detector artifacts fall on this part of the detector, and no decaying latent images from alignment or previous observations are visible in the early frames of each observation or in the undithered stack of the data. A 1.5σ negative "spot" corresponding to a region of known bad pixels at one dither position is observed just below the line. The bad pixels have been masked, but as a result the data at this position only comes from one dither position. This negative spot is likely a sky-subtraction artifact due to a corresponding positive spot visible at the other dither position where the sky was determined. This is not an astrophysical object because the expected dual negative, single positive pattern is not observed. Furthermore, this region varies in intensity in the three-fourths reductions, indicating that it is either a noise fluctuation or a transient effect in the detector. The region does not produce the adjacent positive detection observed for UDFj-39546284 in other masks taken on the same nights.

Despite the positive evidence, this detection should be considered tenuous because 291 other $>2\sigma$ peaks are found between sky lines, 37 of which occur in the full stack and all 4 three-fourths time stacks, and 4 of which have 2 negative detections at the 2 expected dither positions. This places the probability of a chance co-incidence between a noise peak and the reported WFC3 grism observations at between 1% and 86% depending on whether we assume there are 4 or $291 > 2\sigma$ peaks. In addition, the peak is near a sky line increasing the chance of residuals.

Besides UDFj-39546284, we observed four J-dropout, three Y-dropout, and three z-dropout galaxies taken from Ellis et al. (2013) and Schenker et al. (2013) with details noted in Table 1. The goal of including these sources was to search for strong emission lines if the sources were actually at $z < 3$ since all are expected to have Lyα blueward of our spectroscopic range. We find no lines at a sensitivity within 10% of that indicated in Figure 2 placing useful limits for future spectroscopic observations seeking Lyα in the Y and J bands.

3. DISCUSSION

Considering the possibility that UDFj-39546284 is a $z \ll 10$ galaxy, the *HST* observations imply a line flux of 3–$4.7 \times$

10^{-18} erg s^{-1} cm^{-2}. If we combine our 2.2σ flux measurement with the 2.7σ result of Brammer et al. (2013), it results in a 3.5σ detection at 15985.5 ± 4.4 Å with a flux of $1.8 \pm 0.5 \times 10^{-18}$ erg s^{-1} cm^{-2}, at the lower end of what is required to explain the photometry. If we take this combined result at face value along with the photometric analysis of Bouwens et al. (2013), it indicates that UDFj-39546284 is likely at $z \sim 2.19$, and we are seeing the [O III] $\lambda5007$ line. However, at the low significance of our data and that of Brammer et al. (2013), confirmation bias due to coincident noise peaks is problematic and significant unknown systematic effects could be present in both reductions. Furthermore, for typical [O III]/Hβ line ratios of 7.3 in strong line emitting galaxies (Kakazu et al. 2007) one would expect a $>2\sigma$ detection in F140W filter imaging if this source were at $z \sim 2.19$ and this is not observed. In contrast to Brammer et al. (2013), we find that even the extreme object they find with a [O III]/Hβ line ratio of 11.4 should also result in a $\sim2\sigma$ detection assuming the Ellis et al. (2013) photometric limits. The discrepancy is due either to differences in the depths quoted between Brammer et al. (2013) and Ellis et al. (2013), which differ by ~0.4 mag, and/or to how the $z = 1.606$ extreme object photometry and spectra were compared to the UDFj-39546284 limits. In particular, we note the spectral energy distribution shown in Brammer et al. (2013) is not directly comparable to the plotted UDFj-39546284 limits because the filters in the two observations have significantly different bandwidths and the spectral energy distribution is dominated by lines that create significant non-linear flux changes as they redshift through the filter bandpasses. An alternative low-redshift explanation is that we are detecting one of the [O II] $\lambda3727$ doublet lines at $z = 3.29$; however, this is less likely since the [O II] line is typically significantly weaker than the [O III] $\lambda5007$ line. Thus, more data are required before coming to any firm conclusions.

We estimate ~20 hr of integration in good conditions with Keck-I MOSFIRE or an equivalent instrument would confirm the tentative detection at 15985.5 Å at $>5\sigma$, but still be insufficient to detect other lines for typical [O III]/Hβ line ratios in high-equivalent width line emitting galaxies (Kakazu et al. 2007). If the preliminary detection is the strong [O III] $\lambda5006.8$ line at $z = 2.19$, the $\lambda4958.9$ line would be behind a bright sky line and Hβ would be too faint to detect. If instead we are seeing the less likely $\lambda3727$ [O II] doublet at $z = 3.29$, the second line of the doublet would be hidden behind the nearby sky line.

One could also integrate for a similar amount of time in the K band, and attempt to detect the Hα line if the source is at $z = 2.19$ or both of the [O III] lines if the source is at $z = 3.29$.

Assuming our preliminary detection is real, all three of these lines fall between sky lines and should be detectable at $>5\sigma$ for typical line ratios. This may be a more productive approach since it can differentiate between $z = 2.19$, 3.29, and 12.14.

Spectroscopic confirmation with ALMA would be expensive. Assuming this source is at $z \sim 12$, is unobscured, and all of the continuum flux is due to star formation, the expected [CII] 158 μm luminosity would be $\sim$50 μJy assuming 1% of the bolometric luminosity is emerging in this line. With full ALMA, this would require $\sim$72 hr of integration in one receiver tuning to detect at 5σ. However, a non-detection would not confirm a low redshift because of the intrinsic scatter in bolometric luminosity to [CII] line ratio.

If UDFj-39546284 is at high redshift, we expect no detection in the longer spectra and it is unlikely that any conclusive spectra can be obtained with current instrumentation. The typical equivalent width of Lyα in $4 < z < 6$ galaxies is $\sim$20 Å with a tail out to $\sim$80 Å and is expected to decrease at $z \sim 6$–12 due to the increasing opacity of the intergalactic medium (IGM; Stark et al. 2011; Mallery et al. 2012). Assuming UDFj-39546284 is at $z \sim 12$, our flux limit would require a Lyα equivalent width of $\geqslant$200 Å to yield a 2.2σ detection. This large an equivalent width is occasionally observed in the $z \sim 4$–6 universe, but less likely at $z \sim 12$ where the IGM is expected to be more absorptive. For a normal equivalent width of ~ 20 Å, $\sim$460 hr of observation with Keck-I MOSFIRE would be required to detect this galaxy, and even an adaptive optics assisted 30 m class telescope would require $\sim$16 hr of integration.

4. CONCLUSIONS

Using the Keck-I MOSFIRE infrared spectrograph, we recover the 2.7σ line detection reported in Brammer et al. (2013) at the 2.2σ level. Combining these results, we find the 3.5σ line at 15985.5 ± 4.4 Å with an estimated flux of $1.8 \pm 0.5 \times 10^{-18}$ erg s^{-1} cm^{-2}, but the likelihood that this is a chance coincidence of noise peaks is non-negligible, so further observations are needed. If confirmed, the detection indicates UDFj-39546284 is actually a low-redshift line emitter at $z \sim$ 2.19 or 3.29, so both H- and K-band spectra should be obtained to uniquely determine its redshift. If the source is at $z \sim 12$, it is unlikely that ground-based 8–10 m telescopes or ALMA could confirm it and additional data will yield a non-detection. The difficulty in interpreting this source and the high likelihood that it is actually at low redshift highlights the need for spectroscopic studies at $6 < z < 8$ to understand possible sources of contamination at even higher redshifts.

REFERENCES

Atek, H., Siana, B., Scarlata, C., et al. 2011, ApJ, 743, 121
Bouwens, R. J., Illingworth, G. D., Franx, M., & Ford, H. 2007, ApJ, 670, 928
Bouwens, R. J., Illingworth, G. D., Labbe, I., et al. 2011a, Natur, 469, 504
Bouwens, R. J., Illingworth, G. D., Oesch, P. A., et al. 2010, ApJL, 709, L133
Bouwens, R. J., Illingworth, G. D., Oesch, P. A., et al. 2011b, ApJ, 737, 90
Bouwens, R. J., Oesch, P. A., Illingworth, G. D., et al. 2013, ApJL, 765, L16
Brammer, G. B., van Dokkum, P. G., Illingworth, G. D., et al. 2013, ApJL, 765, L2
Bunker, A. J., Caruana, J., Wilkins, S. M., et al. 2013, MNRAS, 430, 3314
Capak, P., Mobasher, B., Scoville, N. Z., et al. 2011, ApJ, 730, 68
Cardamone, C. N., van Dokkum, P. G., Urry, C. M., et al. 2010, ApJS, 189, 270
Caruana, J., Bunker, A. J., Wilkins, S. M., et al. 2012, MNRAS, 427, 3055
Cowie, L. L. 1988, in Proc. NATO Advanced Study Institute, Post-Recombination Universe, ed. N. Kaiser & A. N. Lasenby (Dordrecht: Kluwer), 1
Ellis, R. S., McLure, R. J., Dunlop, J. S., et al. 2013, ApJL, 763, L7
Hayes, M., Laporte, N., Pelló, R., Schaerer, D., & Le Borgne, J.-F. 2012, MNRAS, 425, L19
Iwata, I., Ohta, K., Tamura, N., et al. 2003, PASJ, 55, 415
Kakazu, Y., Cowie, L. L., & Hu, E. M. 2007, ApJ, 668, 853
Mallery, R. P., Mobasher, B., Capak, P., et al. 2012, ApJ, 760, 128
McLean, I. S., Steidel, C. C., Epps, H., et al. 2010, Proc. SPIE, 7735, 77351E
McLean, I. S., Steidel, C. C., Epps, H. W., et al. 2012, Proc. SPIE, 8446, 84460J
McLure, R. J., Dunlop, J. S., Bowler, R. A. A., et al. 2013, MNRAS, 432, 2696
Oesch, P. A., Bouwens, R. J., Carollo, C. M., et al. 2010, ApJL, 709, L21
Oesch, P. A., Bouwens, R. J., Illingworth, G. D., et al. 2012, ApJ, 745, 110
Ono, Y., Ouchi, M., Mobasher, B., et al. 2012, ApJ, 744, 83
Ouchi, M., Shimasaku, K., Okamura, S., et al. 2004, ApJ, 611, 660
Robertson, B. E., Ellis, R. S., Dunlop, J. S., McLure, R. J., & Stark, D. P. 2010, Natur, 468, 49
Schenker, M. A., Robertson, B. E., Ellis, R. S., et al. 2013, ApJ, 768, 196
Stark, D. P., Ellis, R. S., Chiu, K., Ouchi, M., & Bunker, A. 2010, MNRAS, 408, 1628
Stark, D. P., Ellis, R. S., & Ouchi, M. 2011, ApJL, 728, L2
Steidel, C. C., Adelberger, K. L., Giavalisco, M., Dickinson, M., & Pettini, M. 1999, ApJ, 519, 1
Steidel, C. C., Giavalisco, M., Pettini, M., Dickinson, M., & Adelberger, K. L. 1996, ApJL, 462, L17
Steidel, C. C., Hunt, M. P., Shapley, A. E., et al. 2002, ApJ, 576, 653
van der Burg, R. F. J., Hildebrandt, H., & Erben, T. 2010, A&A, 523, A74
Vanzella, E., Giavalisco, M., Dickinson, M., et al. 2009, ApJ, 695, 1163
Vanzella, E., Pentericci, L., Fontana, A., et al. 2011, ApJL, 730, L35